AJNR

Arterial Spin-Labeling Perfusion Imaging in the Early Stage of Sturge-Weber Syndrome

G. Pouliquen, L. Fillon, V. Dangouloff-Ros, M. Kuchenbuch, C. Bar, N. Chemaly, R. Levy, C.-J. Roux, A. Saitovitch, J. Boisgontier, R. Nabbout and N. Boddaert

AJNR Am J Neuroradiol 2022, 43 (10) 1516-1522
doi: https://doi.org/10.3174/ajnr.A7643
http://www.ajnr.org/content/43/10/1516

Arterial Spin-Labeling Perfusion Imaging in the Early Stage of Sturge-Weber Syndrome

G. Pouliquen, L. Fillon, V. Dangouloff-Ros, M. Kuchenbuch, C. Bar, N. Chemaly, R. Levy, C.-J. Roux, A. Saitovitch, J. Boisgontier, R. Nabbout, and N. Boddaert

ABSTRACT

BACKGROUND AND PURPOSE: Sturge-Weber syndrome is a rare congenital neuro-oculo-cutaneous disorder. Although the principal mechanism of Sturge-Weber syndrome is characterized by a leptomeningeal vascular malformation, few data regarding perfusion abnormalities of the brain parenchyma are available. Therefore, the aim of this study was to assess the diagnostic performance of arterial spin-labeling perfusion imaging in the early stage of Sturge-Weber syndrome before 1 year of age until 3.5 years of age. We hypothesized that a leptomeningeal vascular malformation has very early hypoperfusion compared with controls with healthy brains.

MATERIALS AND METHODS: We compared the CBF using arterial spin-labeling perfusion imaging performed at 3T MR imaging in the brain parenchymal regions juxtaposing the leptomeningeal vascular malformation in patients with Sturge-Weber syndrome ($n = 16$; 3.5 years of age or younger) with the corresponding areas in age-matched controls with healthy brains ($n = 58$). The analysis was performed following two complementary methods: a whole-brain voxel-based analysis and a visual ROI analysis focused on brain territory of the leptomeningeal vascular malformation.

RESULTS: Whole-brain voxel-based comparison revealed a significant unilateral decrease in CBF localized in the affected cortices of patients with Sturge-Weber syndrome ($P < .001$). CBF values within the ROIs in patients with Sturge-Weber syndrome were lower than those in controls (in the whole cohort: median, 25 mL/100g/min, versus 44 mL/100g/min; $P < .001$). This finding was also observed in the group younger than 1 year of age, emphasizing the high sensitivity of arterial spin-labeling in this age window in which the diagnosis is difficult.

CONCLUSIONS: Arterial spin-labeling perfusion imaging in the early stage of Sturge-Weber syndrome can help to diagnose the disease by depicting a cortical hypoperfusion juxtaposing the leptomeningeal vascular malformation.

ABBREVIATIONS: ASL = arterial spin-labeling; AUC = area under the curve; FWE = family-wise error; IQR = interquartile range; LVM = leptomeningeal vascular malformation; MNI = Montreal Neurological Institute; PWB = port-wine birthmark; SWS = Sturge-Weber syndrome

Sturge-Weber syndrome (SWS) is a congenital disorder characterized by a triad, variably including an ipsilateral port-wine birthmark (PWB) typically involving the forehead, a leptomeningeal vascular malformation (LVM), and ocular abnormalities.[1-3]

A sporadic, somatic activating mutation in the *GNAQ* gene leads to cell proliferation and inhibition of apoptosis leading to an SWS spectrum.[2,4] Depending on the time in development when the mutation occurs, it may simply provoke PWB or SWS.[2] The main progressive symptoms include seizures, neurodevelopmental delay, and visual defects.[5]

Because the isolated PWB is not referred to as SWS, the brain involvement confirms the diagnosis[5] and may be detected in infants with a high-risk PWB, even before the onset of neurologic symptoms.[6] 3T MR imaging is the primary technique recommended[7] for the diagnosis by the visualization of the LVM on post-contrast-weighted images.[3,5] Other MR imaging signs provide indirect evidence of LVM: ipsilateral choroid plexus enlargement, cerebral atrophy, and signal inversion of the affected WM on T2WI.[3]

Few studies regarding brain perfusion abnormalities are available.[8-18] The latest studies were performed using T2* dynamic

Received February 20, 2022; accepted after revision July 27.

From the Department of Pediatric Radiology (G.P., V.D.-R., R.L., C.-J.R., N.B.) and Centre de Reference Epilepsies Rares (M.K., C.B., N.C., R.N.), Department of Pediatric Neurology, Necker Children's Hospital, Assistance Publique-Hôpitaux de Paris, Université de Paris, Paris, France; and Imagine Institute for Genetic Diseases (G.P., L.F., V.D.-R., R.L., C.-J.R., A.S., J.B., R.N., N.B.), L'Institut National de la Santé et de la Recherche Médicale U1163, Paris, France.

R. Nabbout and N. Boddaert contributed equally to this work

Please address correspondence to Geoffroy Pouliquen, MD, Department of Pediatric Radiology, Necker Children's Hospital, Assistance Publique-Hôpitaux de Paris, University of Paris, 149 Rue de Sèvres, 75015 Paris, France; e-mail: geoffroy.pouliquen@gmail.com

http://dx.doi.org/10.3174/ajnr.A7643

susceptibility contrast material–enhanced imaging, which does not reflect the routine practice in children in expert centers currently. Its application has been limited due to reduced patient comfort and technical difficulties required by high-flow injection of contrast media in small veins.[19]

Arterial spin-labeling (ASL) is a perfusion imaging technique that does not require injection, making it suitable for pediatric patients.[20] Our aim was to assess the diagnostic performance of ASL in the early stage of SWS before 1 year of age until 3.5 years of age by comparing cortical perfusion juxtaposing the LVM with the corresponding areas in controls with healthy brains. We hypothesized that LVM shows an early hypoperfusion compared with controls with healthy brains and investigated this hypothesis following 2 methods: a whole-brain voxel-based analysis and an ROI analysis focused on the brain territory of LVM.

MATERIALS AND METHODS

Subjects

We retrospectively reviewed patients with a confirmed diagnosis of SWS followed at our institution from May 2015 to March 2021. They were recruited from the pediatric neurology department using the full-text search engine database DR WAREHOUSE (https://www.trademarkelite.com/trademark/trademark-detail/87158029/DR-WAREHOUSE).[21] Inclusion criteria were a confirmed diagnosis of SWS in children between 0 and 3.5 years of age obtained on 3T MR imaging during the interictal period with a routine protocol including ASL. Patients were excluded from the study if MR imaging revealed an atypical SWS syndrome (eg, including diagnostic uncertainty or association with other diseases such as scaphocephaly, subdural hematoma, or subarachnoid cyst) or was compromised by artifacts. Age-matched controls were included with the following criterion: examination for various reasons during the time of the study with scans with strictly normal findings (nonexhaustively morphologic evaluation of upper-limit head circumference, feeding difficulties, abnormal eye movements, benign nystagmus, isolated strabismus).

Analyses were performed for the whole cohort and in age groups before or after 1 year of age to focus on young patients when the SWS diagnosis was peculiarly difficult. According to local regulations, institutional review board approval was not required because this was a retrospective study using anonymized data. Consent was waived for this retrospective analysis.

Data Acquisition

Images were acquired in the Department of Pediatric Radiology on a 3T MR imaging scanner (Discovery MR750; GE Healthcare). The standard routine protocol included a 3D T1WI with and without postgadolinium acquisitions, T2WI, FLAIR, SWI, and ASL perfusion imaging.

ASL images were obtained with a 3D pseudocontinuous ASL sequence using an FSE acquisition with spiral filling of the *k*-space and the following parameters: TR = 4453 ms; TE = 10.96 ms; 8 spiral arms in each 3D partition with 512 points per arm; labeling duration = 1500 ms; postlabeling delay = 1025 ms; flip angle = 155°; resolution in plane = 1.875 × 1.875 mm; section thickness = 4 mm; FOV = 240 × 240 mm; acquisition time = 4 minutes 17 seconds.

The standard routine protocol included sedation using intrarectal pentobarbital (5 mg/kg of the child's weight, <20 kg) to avoid motion artifacts in children younger than 5 years of age. In this study, all children (patients and controls) were sedated.

Data Processing

For the data preprocessing and statistical analysis, we used the rest CBF quantification produced automatically by the processing console (GE Healthcare) using a proton-density image for signal normalization during CBF quantification.[22]

Whole-Brain Voxel-Based Analysis

Images were analyzed using Statistical Parametric Mapping 12 (SPM12; http://www.fil.ion.ucl.ac.uk/spm) and Matlab R2018b (MathWorks). Native T1WIs were segmented into GM, WM, and CSF maps using the Computational Anatomy Toolbox 12 (http://www.neuro.uni-jena.de/cat/) in SPM12. Deformation fields between native space and the Montreal Neurological Institute (MNI) space were obtained in this step. The MNI template used for tissue segmentation has been adapted according to the age of the given subject: a pediatric template created with Template-O-Matic toolbox[23] using the National Institutes of Health Pediatric MRI Data Repository (https://www.nitrc.org/projects/pediatric_mri/) for children older than 1 year of age, and the Infant Brain Probability Templates[24] for children younger than 1 year of age.

For each child, the coregistration between the native CBF image and the native GM image was estimated. Then, the combination of the deformation fields and the estimated coregistration was applied to the CBF image to spatially normalize this image in the MNI space with an in-plane resolution of 1.5 × 1.5 mm and a section thickness of 1.5 mm. The resulting image was checked for proper registration and smoothed with a Gaussian kernel of 6-mm full width at half-maximum.

Leptomeningeal Vascular Malformation Analysis

Images were analyzed using a medical image viewer (Vue PACS, Version 12.1.6.0117; Carestream Health). A 2D ROI was manually placed on CBF images in the LVM location for each patient with SWS found on T1-weighted contrast-enhanced images. Similarly, ROIs were placed in the corresponding areas in controls. They were round, with a mean area of 50 mm^2 (range, 40–60 mm^2). Figure 1 displays an illustration of an MR imaging from a patient with SWS.

Statistical Analysis

Whole-Brain Voxel-Based Analysis. For each subgroup, comparisons between children with SWS and controls were performed to investigate voxelwise cortical perfusion differences using a 2-sample *t* test design in the framework of the FSL General Linear Model (http://fsl.fmrib.ox.ac.uk/fsl/fslwiki/GLM). All results were thresholded with a *P* value of .001. Because we had an a priori hypothesis concerning the location of the LVM, we showed the results without the family-wise error (FWE) correction. When significant, results with the FWE correction were also indicated.

LVM-Focused Analysis. CBF values in the angioma ROI for patients and in the corresponding areas for controls were reported as median and interquartile range (IQR). Comparisons

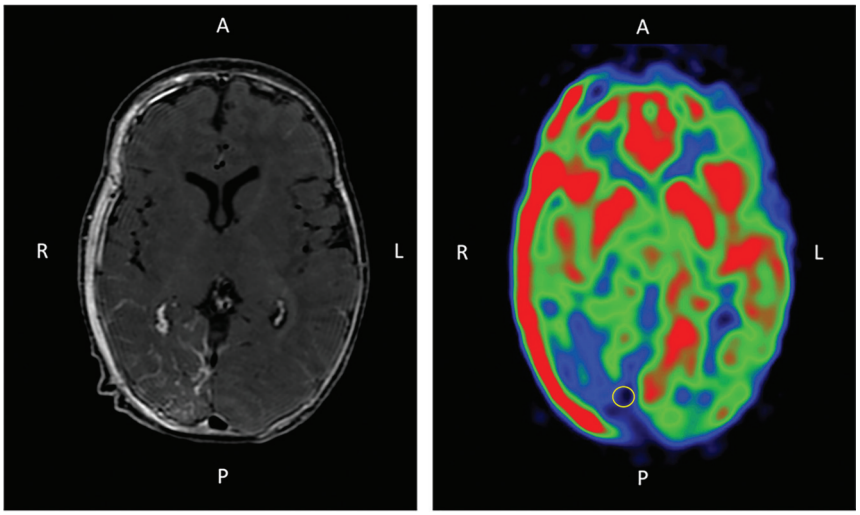

FIG 1. Illustration of a 3-month-of-age patient with SWS with a right occipito-temporo-parietal LVM. Axial slices of the brain on T1-weighted imaging after contrast injection (*left*) and ASL perfusion imaging (*right*) show, respectively, the contrast enhancement and the hypoperfusion associated with the LVM. A ROI (*yellow circle*) was placed in the cortical area juxtaposing the LVM on ASL. Note that an osseous angioma is also present and responsible for the hyperperfused area of the right part of the skull. A indicates anterior; P, posterior; R, right; L, left.

between children with SWS and controls were performed to investigate perfusion differences using Wilcoxon tests. $P \leq .05$ was considered statistically significant.

To explore the diagnostic accuracy of these ROIs to diagnose SWS, we performed receiver operating characteristic curves per age and in the whole cohort; the area under the curve (AUC) was computed, as well as sensitivities and specificities. A bootstrap method was used to calculate the 95% CI of the AUC, sensitivities, and specificities.

RESULTS

Patients

Sixteen patients with 26 scans were identified for this study. Seventeen scans were obtained in children younger than younger than 1 year of age, and 9 scans, in children between 1 and 3.5 years of age. The demographic details of the patients are listed in Table 1. Fifty-eight controls with healthy brains were identified with 25 younger than 1 year of age and 33 from 1 to 3.5 years of age.

Subjects were divided into 4 subgroups based on age and lateralization of the disease. There were 2 subgroups of children younger than 1 year of age with the following: 1) left LVM with 7 examinations, and 2) right LVM with 10 examinations both compared with the 25 controls younger than 1 year of age. There were 2 subgroups of children between 1 and 3.5 years of age with the following: 1) left LVM with 2 examinations, and 2) right LVM with 9 examinations, both compared with the 33 controls with the same age interval. Two patients with bilateral LVMs were included and allocated twice, depending on their age, to the subgroups left and right, independently.

Whole-Brain Voxel-Based Comparisons

For each subgroup, whole-brain voxel-based comparison between CBF in patients with SWS and controls with healthy brains revealed a significant unilateral decrease in CBF localized on the affected cortex of patients with SWS ($P < .001$). Figure 2 shows the

Table 1: Demographics and morphologic imaging data of patients with SWS

Patient	Sex	Examination Age[a] (months)	Leptomeningeal Vascular Malformation		Epilepsy	Atrophy	Calcifications
			Side	Extension (Lobe)			
1	Female	3	Left	FTP	None	None	None
2	Female	0/11	Bilateral	LO/RO	None	None	None
3	Female	0/9	Left	OT	None	None	None
4	Male	1	Left	HS	None	None	Present
5	Male	11	Left	OP	None	None	None
6	Female	1	Right	O	None	None	None
7	Female	2/25	Right	O	Present	None	None
8	Male	3/18	Right	OTP	Present	Present	Present
9	Female	4/6/17	Right	HS	Present	Present	Present
10	Female	4/11	Right	O	None	None	None
11	Male	9	Right	OTP	None	None	None
12	Female	27	Left	O	Present	None	Present
13	Female	42	Bilateral	LFP/ROTP	Present	None	None
14	Male	16	Right	OTP	Present	Present	Present
15	Male	18	Right	O	Present	None	Present
16	Male	30	Right	O	None	None	None

Note:—F indicates frontal; O, occipital; HS, hemisphere; OP, occipito-parietal; OTP, occipito-temporo-parietal; LFP, left fronto-parietal; ROTP, Right occipito-temporo-parietal; FTP, fronto-temporo-parietal; LO, left occipital; RO, right occipital; OT, occipito-temporal.

[a] Two or 3 numbers are reported in this column when several examinations were performed for the same patient.

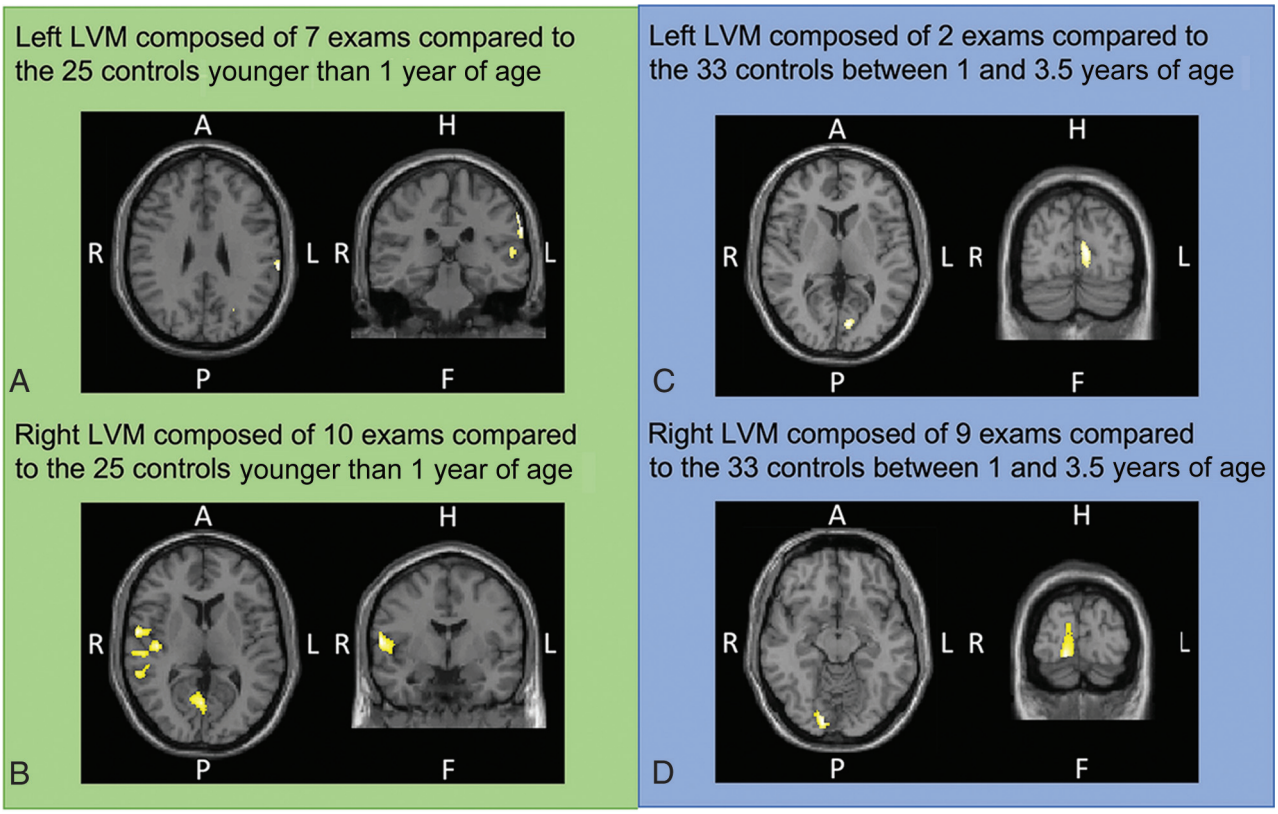

FIG 2. Whole-brain voxel-by-voxel SPM analyses in children with SWS and controls with healthy brains younger than 1 year of age (*A* and *B*) and from 1 to 3.5 years of age (*C* and *D*). Templates are shown with the radiologic convention in the axial and coronal plains. Significant hypoperfusion is labeled by *yellow areas*. A indicates anterior; P, posterior; H, head; F, foot; L, left; R, right.

Table 2: CBF in LVM of patients with SWS and corresponding area in controls

CBF (mL/100g/min)	Patients (Median) (IQR)	Controls (Median) (IQR)	Wilcoxon *P*
A, Left, younger than 1 year of age	17 (13–33)	41 (33–47)	.02
B, Right, younger than 1 year of age	23 (20–29)	38 (32–45)	.01
C, Left, between 1 and 3.5 years of age	25 (24–26)	52 (41–62)	.02
D, Right, between 1 and 3.5 years of age	28 (13–33)	48 (39–64)	.003
Whole cohort	25 (14–30)	44 (34–55)	<.0001

significant hypoperfusion areas, depending on the analyzed subgroup. Children with SWS who were younger than 1 year of age with a left LVM (Fig 2*A*) had a significant CBF decrease in the left parietotemporal cortex (main cluster: $t = 4.44$; $z_{(score)} = 3.85$; $P_{(uncorrected)} < .001$; MNI coordinates: x = −64, y = −28, $z = 28$). Children with SWS who were younger than 1 year of age with a right LVM (Fig 2*B*) had a significant CBF decrease in the right occipital, temporal cortex (main cluster: $t = 5.07$; $z_{(score)} = 4.31$; $P_{(uncorrected)} < .001$; $P_{(FWE\text{-}corrected\ cluster\text{-}level)} < .001$; MNI coordinates: x = 60, y = −3, z = 8).

Children with SWS between 1 and 3.5 years of age with a left LVM (Fig 2*C*) had a significant CBF decrease in the left parieto-occipital cortex ($t = 4.49$; $z_{(score)} = 3.66$; $P_{(uncorrected)} < .001$; MNI coordinates: x = −8, y = −80, z = 6). Children with SWS between 1 and 3.5 years of age with a right LVM (Fig 2*D*) had a significant CBF decrease in the occipital cortex (main cluster: $t = 5.12$; $z_{(score)} = 4.43$; $P_{(uncorrected)} < .001$; $P_{(FWE\text{-}corrected\ cluster\text{-}level)} = .016$; MNI coordinates: x = 16, y = −90, z = −12).

ROI-Based Analysis

CBF values in the ROIs in patients with SWS were lower than those in controls (in the whole cohort: median, 25 mL/100g/min [IQR = 14–30 mL/100g/min] versus 44 mL/100g/min [IQR = 34–55 mL/100g/min], respectively, $P < .0001$). This significant difference was found for all subgroups regardless of the patient's age and side of the LVM (Table 2 and Fig 3).

Diagnostic Accuracy

As shown in Fig 4, the receiver operating characteristic curve for the whole cohort had an AUC of 0.84 (95% CI, 0.75–0.93). The optimal threshold for the global analysis including all patients and controls was a CBF at 30 mL/100g/min with a specificity of 77% (95% CI, 75–93) and sensitivity of 88% (95% CI, 75–93).

In the subgroup of patients younger than 1 year of age, the AUC was 0.78 (95% CI, 0.63–0.93). A threshold of 36 mL/100g/min yielded a specificity of 89% (95% CI, 67–100) and a sensitivity of 82% (95% CI, 73–91) in this subgroup.

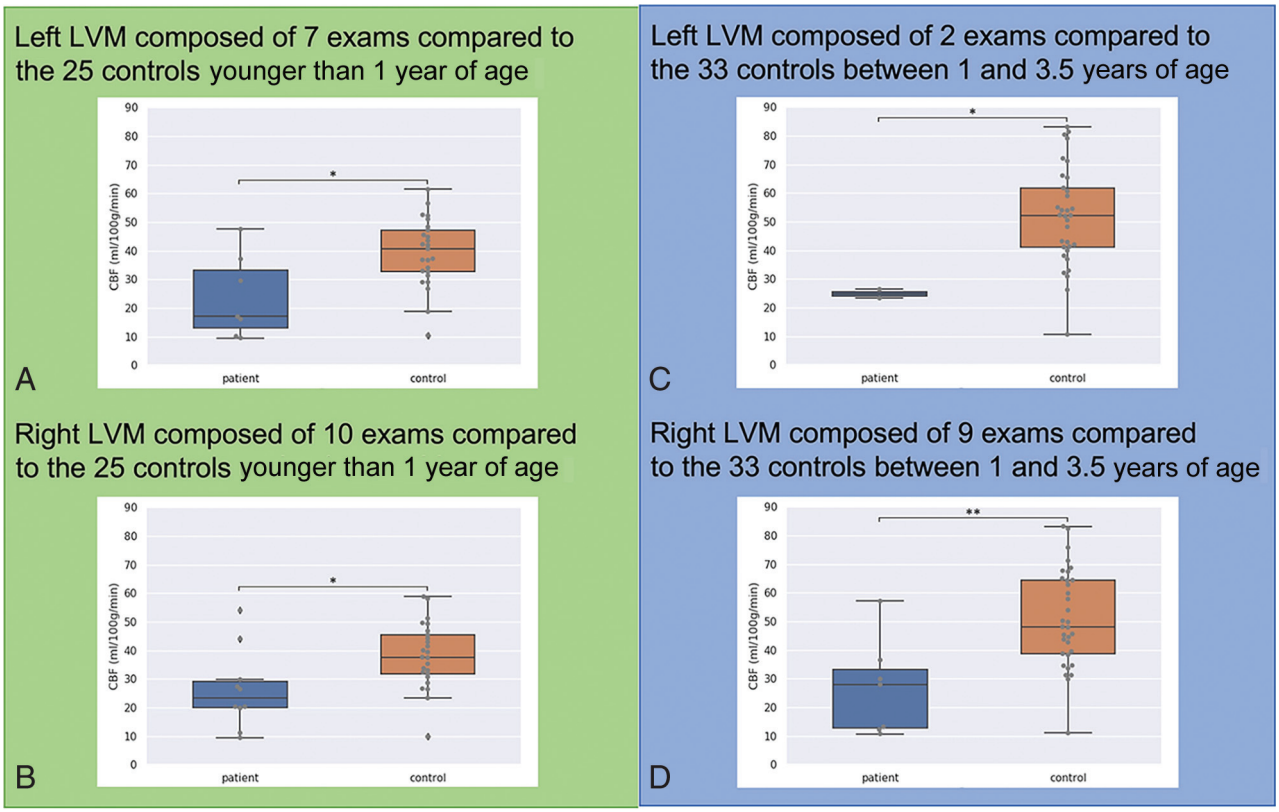

FIG 3. Comparison of CBF values between LVMs in children with SWS and corresponding areas in controls for subgroups matched for age and side. Horizontal bars on the top of the graphs show significant differences. *Asterisk* indicates $P < .05$; *double asterisks*, $P < .01$.

DISCUSSION

In this series of 16 young patients with SWS (3.5 years of age or younger), ASL perfusion imaging had a cortical hypoperfusion juxtaposing the LVM compared with pair-wise controls. This finding was observed in the group younger than 1 year of age, emphasizing the high sensitivity of ASL in this age window in which the diagnosis is difficult. These results were not driven by atrophy or calcification of the diseased cortex. Each subgroup showed a significant hypoperfusion including the subgroup in which no patient had cortical atrophy. In the same way, it was unlikely driven by calcifications because in the age group younger than 1 year, only 3 patients of 11 had calcifications.

Such findings are in line with histologic studies. The cortical blood flow reduction could have been speculated as secondary to the venous stasis and hypertension due to malformation of the cortical vessels as well as venous thrombosis leading to impaired cortical perfusion and ischemia.[17] In our study, the brain hypoperfusion corresponding to the LVM was unchanging during development up to 3.5 years of age and did not show the normal cortical maturation increasing with age.[20]

Data in the literature reported the role of brain perfusion to unravel the difficulty of detection of LVM,[8,10-16] which can be slight or discrete at an early stage. Our results were consistent because these studies have demonstrated decreased perfusion in the parenchyma regions juxtaposing the leptomeningeal enhancement. Whitehead et al[25] reported hypoperfusion in 2 patients with SWS without leptomeningeal abnormalities. All patients in our cohort with obvious hypoperfusion also had leptomeningeal enhancement.

Presymptomatic use and optimal timing of MR imaging in the investigation of PWB have been controversial issues.[1] A recent expert consensus concluded that for neonates and infants with a high-risk PWB and no history of seizures or neurologic symptoms, routine screening for brain involvement was not recommended; MR imaging should be reserved for symptomatic infants or children.[6] This guidance was mainly based on 2 observations: First, negative findings on neuroimaging in a normally developing asymptomatic infant with a facial PWB do not exclude brain involvement and may provide false reassurance. Such false-negative findings have been reported in 3%–23% of the cases in retrospective studies.[6] Second, even if an LVM is confirmed, neurologically asymptomatic children are unlikely to undergo immediate therapeutic intervention.[6] Nevertheless, other reasons drive pediatric neurologists to perform early MR imaging, including parental expectations, anxieties, or discomfort with diagnostic uncertainty.[1] It also may be performed to confirm the pathology when an atypical presentation is encountered or to exclude a differential diagnosis that includes variable and overlapping phenotypes such as *PIK3CA*-related disorders with no decreased CBF. This consensus was built on a literature review from 2008 to 2018, so it could not take into consideration 2 recent studies.

Bar et al[3] reported that leptomeningeal enhancement invisible before 1 year of age may appear afterward and proposed an MR imaging protocol to diagnose SWS during the presymptomatic stage in this difficult age window, obtaining a sensitivity of 100% and a

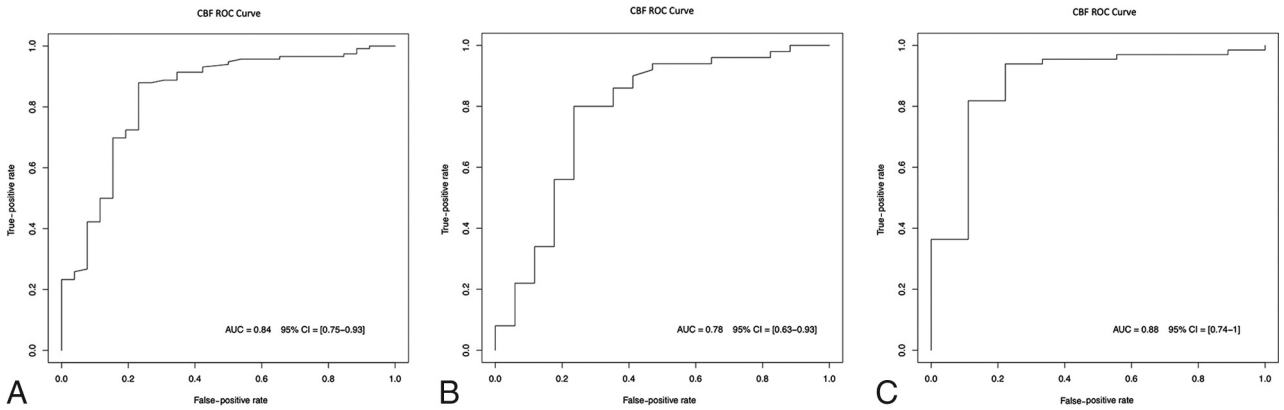

FIG 4. Receiver operating characteristic (ROC) curves for the whole cohort (*A*), patients younger than 1 year of age (*B*), and patients older than 1 year of age (*C*).

specificity of 94%. Day et al[26] assessed the presymptomatic treatment before seizure onset in SWS compared with postsymptomatic treatment on pair-wise subjects. By reducing seizure scores in presymptomatically treated subjects, they hypothesized that prophylaxis may delay seizure onset. These studies put in perspective the possible key role of imaging to early and presymptomatically detect LVM, while waiting for more evidence of the benefit of early and presymptomatic treatment. Hypoperfusion detected on ASL in our study (decreased around 20 mL/100g/min in comparison with age-matched controls) may either help to increase vigilance in children younger than 1 year of age suspected of having SWS if there is a doubtful LVM enhancement, or may increase confidence to diagnose the LVM. This ASL sign could be added to indirect MR imaging anatomic signs already described by Bar et al[3] to detect the LVM in this difficult age window before the age of 1 year. Larger prospective cohorts with serial MR imaging in the same patients are warranted to assess the time course of perfusion abnormalities and other MR imaging signs.

Limits in our study should be mentioned. The study had a small sample size effect, which prevented sound analysis of small subgroups. Moreover, considering the small sample size of our diseased group, several scans from some patients were considered independently, introducing a representation bias. The advantage of a voxelwise analysis was to display a global tendency among the studied individuals. However, because it takes into consideration the average perfusion of all subjects while they had a different brain expression, the analysis mixed LVM and healthy brain areas, resulting in an averaging effect. Therefore, the abnormality-focused analysis using an ROI was complementary because the measured CBF in each patient was not averaged by others who had a different location of the disease. Finally, patients who did not have a concomitant electroencephalogram and had subtle nonmotor seizures during the ASL acquisition, though not the most frequent type in this population, could have been unnoticed.

CONCLUSIONS

ASL perfusion imaging may help to diagnose SWS during the early stage by showing a cortical hypoperfusion and could be very useful before the age of 1 year. This ASL sign could be added to other MR imaging signs already described to detect the LVMs in this difficult age window. Even if the place of screening and prophylactic treatment to prevent the seizure onset still needs to be clarified, ASL perfusion imaging gives valuable information about LVMs without the injection of contrast media. Included in an adapted MR imaging protocol, it could promote the MR imaging screening for SWS.

Disclosure forms provided by the authors are available with the full text and PDF of this article at www.ajnr.org.

REFERENCES

1. Zallmann M, Leventer RJ, Mackay MT, et al. **Screening for Sturge-Weber syndrome: a state-of-the-art review.** *Pediatr Dermatol* 2018; 35:30–42 CrossRef Medline
2. Silverstein M, Salvin J. **Ocular manifestations of Sturge-Weber syndrome.** *Curr Opin Ophthalmol* 2019;30:301–05 CrossRef Medline
3. Bar C, Pedespan JM, Boccara O, et al. **Early magnetic resonance imaging to detect presymptomatic leptomeningeal angioma in children with suspected Sturge-Weber syndrome.** *Dev Med Child Neurol* 2020;62:227–33 CrossRef Medline
4. Shirley MD, Tang H, Gallione CJ, et al. **Sturge-Weber syndrome and port-wine stains caused by somatic mutation in *GNAQ*.** *N Engl J Med* 2013;368:1971–79 CrossRef Medline
5. Comi AM. **Sturge-Weber syndrome.** *Handb Clin Neurol* 2015; 132:157–68 CrossRef Medline
6. Sabeti S, Ball KL, Bhattacharya SK, et al. **Consensus Statement for the Management and Treatment of Sturge-Weber Syndrome: Neurology, Neuroimaging, and Ophthalmology Recommendations.** *Pediatr Neurol* 2021;121:59–66 CrossRef Medline
7. De la Torre AJ, Luat AF, Juhász C, et al. **A multidisciplinary consensus for clinical care and research needs for Sturge-Weber syndrome.** *Pediatr Neurol* 2018;84:11–20 CrossRef Medline
8. Riela AR, Stump DA, Roach ES, et al. **Regional cerebral blood flow characteristics of the Sturge-Weber syndrome.** *Pediatr Neurol* 1985; 1:85–90 CrossRef Medline
9. Pinton F, Chiron C, Enjolras O, et al. **Early single-photon emission computed tomography in Sturge-Weber syndrome.** *J Neurol Neurosurg Psychiatry* 1997;63:616–21 CrossRef Medline
10. Griffiths PD, Boodram MB, Blaser S, et al. **99mTechnetium HMPAO imaging in children with the Sturge-Weber syndrome: a study of nine cases with CT and MRI correlation.** *Neuroradiology* 1997;39:219–24 CrossRef Medline
11. Maria BL, Neufeld JA, Rosainz LC, et al. **High prevalence of bihemispheric structural and functional defects in Sturge-Weber syndrome.** *J Child Neurol* 1998;13:595–605 CrossRef Medline
12. Maria BL, Neufeld JA, Rosainz LC, et al. **Central nervous system structure and function in Sturge-Weber syndrome: evidence of**

neurologic and radiologic progression. *J Child Neurol* 1998;13:606–18 CrossRef Medline

13. Evans AL, Widjaja E, Connolly DJA, et al. **Cerebral perfusion abnormalities in children with Sturge-Weber syndrome shown by dynamic contrast bolus magnetic resonance perfusion imaging.** *Pediatrics* 2006;117:2119–25 CrossRef Medline
14. Lin DD, Barker PB, Hatfield LA, et al. **Dynamic MR perfusion and proton MR spectroscopic imaging in Sturge-Weber syndrome: correlation with neurological symptoms.** *J Magn Reson Imaging* 2006;24:274–81 CrossRef Medline
15. Yu TW, Liu HM, Lee WT. **The correlation between motor impairment and cerebral blood flow in Sturge-Weber syndrome.** *Eur J Paediatr Neurol* 2007;11:96–103 CrossRef Medline
16. Wu J, Tarabishy B, Hu J, et al. **Cortical calcification in Sturge-Weber syndrome on MRI-SWI: relation to brain perfusion status and seizure severity.** *J Magn Reson Imaging* 2011;34:791–98 CrossRef Medline
17. Miao Y, Juhász C, Wu J, et al. **Clinical correlates of white matter blood flow perfusion changes in Sturge-Weber syndrome: a dynamic MR perfusion-weighted imaging study.** *AJNR Am J Neuroradiol* 2011;32:1280–85 CrossRef Medline
18. Alkonyi B, Miao Y, Wu J, et al. **A perfusion-metabolic mismatch in Sturge-Weber syndrome: a multimodality imaging study.** *Brain Dev* 2012;34:553–56 CrossRef Medline
19. Hales PW, Kawadler JM, Aylett SE, et al. **Arterial spin-labeling characterization of cerebral perfusion during normal maturation from late childhood into adulthood: normal "reference range" values and their use in clinical studies.** *J Cereb Blood Flow Metab* 2014;34:776–84 CrossRef Medline
20. Lemaître H, Augé P, Saitovitch A, et al. **Rest functional brain maturation during the first year of life.** *Cereb Cortex* 2021;31:1776–85 CrossRef Medline
21. Garcelon N, Neuraz A, Salomon R, et al. **A clinician friendly data warehouse oriented toward narrative reports: Dr. Warehouse.** *J Biomed Inform* 2018;80:52–63 CrossRef Medline
22. Zaharchuk G, Bammer R, Straka M, et al. **Arterial spin-label imaging in patients with normal bolus perfusion-weighted MR imaging findings: pilot identification of the borderzone sign.** *Radiology* 2009;252:797–807 CrossRef Medline
23. Wilke M, Holland SK, Altaye M, et al. **Template-O-Matic: a toolbox for creating customized pediatric templates.** *Neuroimage* 2008;41:903–13 CrossRef Medline
24. Altaye M, Holland SK, Wilke M, et al. **Infant brain probability templates for MRI segmentation and normalization.** *Neuroimage* 2008;43:721–30 CrossRef Medline
25. Whitehead MT, Vezina G. **Osseous intramedullary signal alteration and enhancement in Sturge-Weber syndrome: an early diagnostic clue.** *Neuroradiology* 2015;57:395–400 CrossRef Medline
26. Day AM, Hammill AM, Juhász C, et al; National Institutes of Health Sponsor: Rare Diseases Clinical Research Network (RDCRN) Brain and Vascular Malformation Consortium (BVMC) SWS Investigator Group. **Hypothesis: presymptomatic treatment of Sturge-Weber syndrome with aspirin and antiepileptic drugs may delay seizure onset.** *Pediatr Neurol* 2019;90:8–12 CrossRef Medline